Journal of Applied Polymer Science

Motion mode of poly(lactic acid) chains in film during strain-induced crystallization

Zhefeng Chen,[1] Shuyang Zhang,[1] Feng Wu,[1] Wei Yang,[1] Zhengying Liu,[1] Mingbo Yang[1,2]
[1]College of Polymer Science and Engineering, Sichuan University, Chengdu 610065, People's Republic of China
[2]State Key Laboratory of Polymer Materials Engineering, Sichuan University, Chengdu 610065, People's Republic of China
Correspondence to: Z. Liu (E-mail: liuzhying@scu.edu.cn) and M. Yang (E-mail: yangmb@scu.edu.cn)

ABSTRACT: How stress and temperature impact the movement of poly(lactic acid) (PLA) chains in the process of tensile film stretching was studied. The motion mode of chains was investigated through the study of the strain-induced crystallization and orientation through changes in the draw temperature (T_d), draw ratio, and draw rate. The crystallinity and orientation degrees of the PLA films were measured by differential scanning calorimetry, Fourier transform infrared spectroscopy, and polarized optical microscopy. According to the competition between the orientation caused by the stretching and relaxation of chains under the temperature field, the motion modes of PLA chains during strain were divided into four types, modes I–IV. When T_d was 100°C, the PLA chains acted in mode I, in which the relaxation rate of chains was so fast that no crystallinity or orientation could be obtained. Beyond a draw rate of 20 mm/min at a T_d of 90°C, the type of chain movement changed from mode I to II. In mode II, only crystallites could be reserved after unloading. Chains in the PLA film moved in mode III at a T_d of 80°C; then, both the crystallization and orientation were enhanced monophonically with increasing draw rate. Beyond the draw rate of 10 mm/min at a T_d of 70°C, the orientation rate of chains was much faster than the relaxation one, and the motion mode transformed from mode III to IV. Then, obvious decreases in the crystallinity and orientation were observed with further increases in the draw rate; this resulted from the destruction of the crystallites. © 2015 Wiley Periodicals, Inc. J. Appl. Polym. Sci. **2016**, *133*, 42969.

KEYWORDS: crystallization; films; phase behavior

Received 10 July 2015; accepted 23 September 2015
DOI: 10.1002/app.42969

INTRODUCTION

Scholars and the public are paying more and more attention to environmentally friendly materials because of an increasing awareness of sustainable development and environmental protection. Current levels of the usage and disposal of packaging items or other short-lived products have exerted much pressure on the environment. The replacement of petroleum-based packaging materials with biodegradable ones has been considered, and poly(lactic acid) (PLA) is a representative candidate[1–3] because of its reproducibility, biodegradability, and biocompatibility.[4–8]

Some advantages can be shown when PLA is compared to the petroleum-based polymers commonly used for packaging: (1) PLA exhibits a good transparency that is slightly higher than those of poly(ethylene terephthalate) and polystyrene, and (2) PLA can degrade into nontoxic components, such as carbon dioxide, water, and humus,[9] and this could solve environmental waste disposal problems that occur after the useful life of the products is over. Meanwhile, as a biopolymer, PLA has been widely used at the industrial level;[10,11] this makes it possible for manufacturers to meet demands quantitatively. For packaging materials, a strength–toughness balance point and reasonable barrier properties are required. However, because of the rigid chain[12–14] and the slow kinetics of crystallization, there is not enough time for the formation of orientation and crystals in traditional processes such as film blowing. Therefore, the use of these amorphous PLA products as packaging materials is limited because of the normal brittleness, low heat distortion temperature, and relatively poor barrier properties. Efficient strategies for enhancing these mechanical properties and barrier properties include enhancing the interaction between molecular chains, improving the regularity of chain arrangement, and facilitating crystallization during preparation.[15–18] So, considerable efforts should be focused on promoting the crystallization and orientation of PLA, especially in the preparation of PLA films used as packaging materials.

It has been reported that stretching significantly enhances the crystallization and orientation of PLA as well as its heat resistance.[15,19,20] Extensive studies have been done to investigate the evolution of strain-induced crystallization and orientation.[15,21]

Delpouve *et al.*[22] confirmed that the water-barrier properties are determined not only by the crystallinity in PLA films but also by the strain-induced oriented conformation of amorphous chains. Also, macromolecules oriented homogeneously in the film plane lead to the most disturbing effect of the water passage. The crystal forms of PLA induced by stretching and the transition from α to β during the process of deformation have been researched,[22–24] and the results show that a 10/7 helical–3/2 helical transition in the chain conformation occurred. Zhang *et al.*[25,26] found not only would the crystal and orientation of PLA form during drawing process, but also a defectlike cavity would occur in crystal; this resulted from the movement forced by the stretching of the chains. The cavity emerging during deformation may be the critical reason for the brittle properties of PLA. This result was consistent with that of Liu *et al.*[27] Recently, a special strain-induced phase called the *mesophase,* where the degree of order in chain conformation is located between the crystal and amorphous domains, has been observed and investigated during deformation by some scholars.[28–31]

Strain-induced crystallization seems to be an ideal way to promote the crystallization of the PLA matrix. In the meanwhile, the temperature is another important effect that may make rigid chains more active in overcoming the energy barrier of orientation and relaxation movement. It is worth noticing that the film blowing processing for packaging is always accompanied by multiple external stresses and temperature fields. Therefore, it will be meaningful to research the relationship between the motion mode of PLA chains and the synergy of external fields. In this study, the mode of transformation of chain motion in the PLA film was examined.

EXPERIMENTAL

Materials and Film Preparation

A commercial PLLA [trade name REVODE110, kindly supplied by Zhejiang Haizheng, Ltd., China, number-average molecular weight = 5.0 × 10^4 g/mol, weight-average molecular weight = 10.52× 10^4 g/mol, polydispersity index = 2.1, with a 96 mol % L-isomeric content in pellet form, glass-transition temperature (T_g) = 56°C] was used in this study. PLLA pellets were dried at 60°C for 12 h before use. Dried PLA pellets were compression-molded into 50 μm thick films at 200°C; this was followed by quenching to room temperature. Then, perfect amorphous and isotropic films were obtained.

The drawn films were prepared with a Shimadzu AGS-J universal testing machine equipped with a temperature-control chamber. Films for drawing that were 50 mm in length and 10 mm in width were cut out from the compression films. First, the films were drawn to draw ratios (DRs) ranging from 2.5 to 4 at draw temperatures (T_d's) ranging from 70 to 100°C at a crosshead speed of 5 mm/min. Then, the drawn films were quenched to room temperature. Second, at T_d of 80°C, the undrawn films were drawn at rates of extension ranging from 5 to 40 mm/min to a fixed DR of 4. Then, the drawn films were quenched to room temperature as well. Parallel ink marks were printed along the film before extension to calculate the strain (ε):

$$\varepsilon = l/l_o$$

where l and $l_o \approx 5$ mm are the lengths between the marks after and before drawing, respectively.

Fourier Transform Infrared (FTIR) Spectroscopy

The FTIR spectra of the drawn films were obtained with a Nicolet 6700 FTIR instrument from Thermo Electron Corp. The spectra were collected in transmission mode in the region from 4000 to 500 cm^{-1}. The absorbance of IR bands was determined with Omnic software. Two kinds of transmission spectra were collected for each uniaxially drawn film for orientation studies with polarized incident beams parallel and perpendicular to the stretching direction. The IR dichroic ratio (D) was calculated with the following equation:

$$D = A_{\parallel}/A_{\perp}$$

where $A_{\parallel}$ and $A_{\perp}$ are the absorbances that are parallel and perpendicular to the stretching direction, respectively.

Differential Scanning Calorimetry (DSC)

A DSC apparatus (Q20, TA Instruments, Inc.) was used to investigate the thermal properties of the drawn films. Each film was heated from equilibrium of 40–200°C at a heating rate of 10°C/min. Only the first heating cycle of each film was analyzed in this study to determine the melting temperature and the heat of fusion. The degree of crystallinity (X_c) of the films was determined by the following equation:

$$X_c = (\Delta H_m - \Delta H_{cc})/\Delta H_{100}$$

where ΔH_m is the enthalpy of melting, ΔH_{cc} is the enthalpy of cold crystallization, and ΔH_{100} (93 J/g)[32] is the heat of fusion of the completely crystalline PLLA. For isothermal crystallization, the films of neat PLA were first heated to 200°C at a rate of 100°C/min and held for 5 min and then cooled to 90, 100, 105, and 110°C at a rate of 100°C/min to monitor the isothermal crystallization process for 60 min. All of these processes were carried out under a nitrogen atmosphere.

Polarized Optical Microscopy (POM)

An Olympus BX51 polarizing optical microscope (Olympus Co., Tokyo, Japan) equipped with a digital camera was used to investigate the morphology of the condensed state in the PLA films.

Wide-Angle X-ray Diffraction Analysis

Wide-angle X-ray diffraction profiles were recorded on a DX-1000 X-ray diffractometer (Dandong Fanyuan Instrument Co., Ltd.), and a Cu Kα radiation source (λ = 0.154056 nm, 40 kV, 25 mA) was used in a scanning angle range of 2–40° at a scan speed of 3°/min.

RESULTS AND DISCUSSION

Crystallization Significantly Enhanced by Stretching

The FTIR spectra of the drawn films are shown in Figure 1(a). According to the report on the IR band assignments for both the crystal and amorphous phases of PLA, the bands at 697, 739, 921, and 1293 cm^{-1} were attributed to the α-crystalline phase, and those at 710, 757, 895, 956, and 1302 cm^{-1} were attributed to the amorphous phase.[19] We analyzed the bands at 921 cm^{-1} primarily to demonstrate the evolution of the

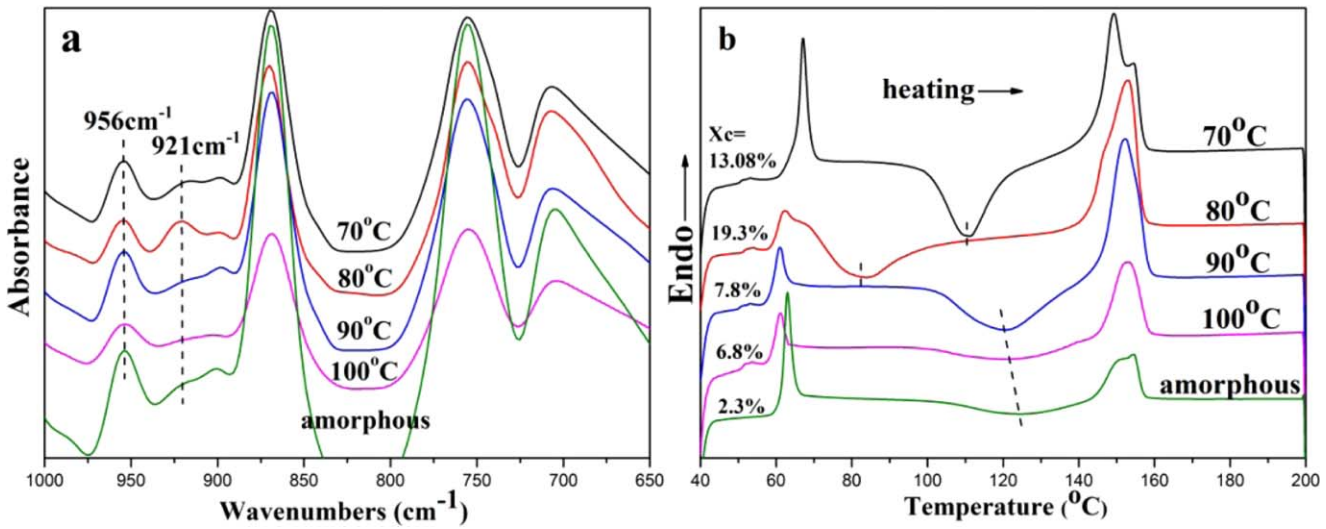

Figure 1. (a) FTIR spectra in the region $1000-650\ cm^{-1}$ and (b) DSC curves of uniaxially drawn films at various temperatures with a draw rate of 5 mm/min and a DR of 4. [Color figure can be viewed in the online issue, which is available at wileyonlinelibrary.com.]

crystalline phase in the PLA film during deformation because the absorbance of the band depended on the amount of crystal and it got stronger with increasing crystallinity. As shown in Figure 1, the absorbance of the band at 921 cm^{-1} of the films drawn at low temperatures (70 and 80°C) was intensely enhanced, but those of the films drawn at high temperatures (90 and 100°C) could not even observed; this means that the crystallization may have occurred in films drawn at low temperatures but not in those drawn at high temperatures when the draw rate was 5 mm/min and DR was 4.

The DSC diagrams are portrayed in Figure 1(b) and the parameters are summarized in Table I to present the crystallinity of the PLA films drawn at different temperatures. Generally, three peaks, corresponding to T_g, cold crystallization, and the melting of crystals, were obtained in the DSC curves of PLA during the heating process. Obviously, the crystallinity of PLA was enhanced dramatically when the samples were drawn at temperatures higher than T_g, according to the peaks of cold crystallization and melting. In addition, the crystallization in the PLA films during the deformation seemed to depend on the value of ΔT where $\Delta T = T_d - T_g$. And the ΔT means the temperature difference between the T_d and T_g here. For example, the crystallization of the film was significantly enhanced at a T_d of 80°C but no so obviously at a T_d of 70°C; moreover, lower crystallinities than that at 70°C were observed at T_d's of 90 and 100°C, as shown in Figure 1. The previously phenomenon was similar to what Mahendrasingam[33] confirmed previously.

It was worth noticing that the cold crystallization temperature (T_{cc}) of the film drawn at 80°C was much lower than those of the films drawn at 70, 90, and 100°C, as shown in Figure 1(b) and Table I. From the previous results, we assumed that a complicated structural transition in the amorphous phase occurred; this was induced by the synergy of deformation and temperature. Thereby, it was necessary to systematically research the reasons for the previous phenomenon; various DRs and rates were used for the tensile testing of the PLA film at each temperature.

Changing Tendencies of Crystallization and Orientation with Various DRs Ranging from 2.5 to 4

The DSC curves of the films drawn to various DRs at a draw rate of 5 mm/min are shown in Figure 2, and the parameters are summarized in Table II. Compared to amorphous films ($X_c = 2.3\%$), at a T_d of 80°C, the crystallinities of the drawn films were enhanced intensely and got higher with increasing DR. A similar phenomenon was observed at a T_d of 70°C, except at a DR of 4, where the crystallinity decreased a little relative to that at a DR of 3.5 ($X_c = 15.1\%$). However, at T_d's of 90 and 100°C, the crystallinities induced by deformation were low and showed slight increases (3.4 and 1.8%, respectively) with the increasing DR. Then, we found that the cold crystallization peaks of all of the drawn films got stronger compared to those of the amorphous ones (Figure 2). This means that some structure, which can enhance the crystallization capacity of PLA chains during the heating process, was induced by strain in the drawn films. In a comparison of the films drawn to the same DR (except the DR of 2.5), the T_{cc} of the film drawn at 70°C was lower than those of films drawn at 90 and 100°C. (At a DR of 2.5, the value of T_{cc} was almost equal to that of the film drawn at 100°C.) In particular, the T_{cc} of the film drawn at 80°C was the lowest one. In addition, as a function of DR, T_{cc} got lower and lower with increasing DR for the films drawn at T_d's of 70 and 80°C. However, the T_{cc} of the film drawn at 90°C showed a slight decrease with increasing DR. At 100°C, T_{cc} seemed to be independent of DR. The reasons driving the T_{cc} of films to lower temperatures was assumed to be the orientation of chains and/or crystals induced by strain at T_d's of 70 and

Table I. DSC Parameters of Uniaxially Drawn Films at Various Temperatures with a Draw Rate of 5 mm/min and with a DR of 4

T_d (°C)	70	80	90	100	Amorphous
T_{cc} (°C)	111.2	83.7	120.6	120	124.5
X_c (%)	13.08	19.3	7.8	6.8	2.3

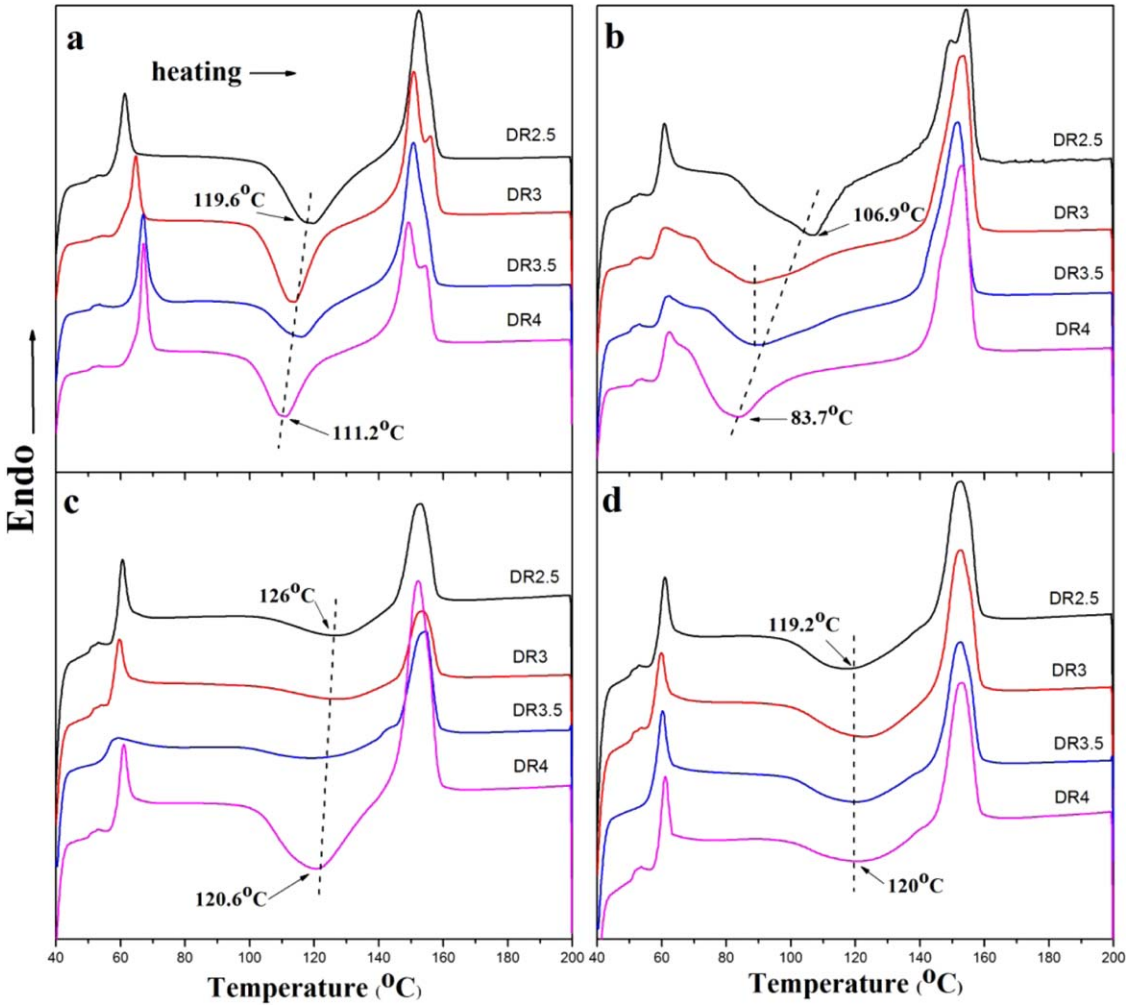

Figure 2. DSC heating curves of uniaxially drawn films with a draw rate of 5 mm/min and various DRs at different T_d values: (a) 70, (b) 80, (c) 90, and (d) 100°C. [Color figure can be viewed in the online issue, which is available at wileyonlinelibrary.com.]

80°C. These new structures induced by strain could promote the crystallization ability in the heating process; namely, oriented chains formed during deformation were more easily crystallized than those random chains in the amorphous phase of PLA when the film was heated; Meanwhile or alternatively, the crystallites formed during deformation existing in the drawn PLA films could perform as nucleating agents during the heating process. To investigate the reason causing the changing in T_{cc}, more information about the chain orientation should be obtained.

The amorphous and crystalline orientations in the drawn films were measured by the IR dichroic with FTIR spectroscopy, and the data are summarized in Table II. As shown in Figure 3(a), the degrees of amorphous orientation of the films drawn at T_d's of 70 and 80°C increased monotonically with increasing DR. However, at a T_d of 70°C, the crystallinity of the drawn film at

Table II. DSC and FTIR Parameters of Films Drawn at a Draw Rate of 5 mm/min

	X_c (%)		T_{cc} (°C)		Dichroic ratio in the amorphous phase	
T_d (°C)	DR = 2.5	DR = 4	DR = 2.5	DR = 4	DR = 2.5	DR = 4
70	2.4	13.08	119.6	111.2	1.267	1.701
80	10.1	19.3	106.9	83.7	1.155	1.568
90	4.4	7.8	126	120.6	1.05	1.053
100	5	6.8	119.2	120	1.049	1.035

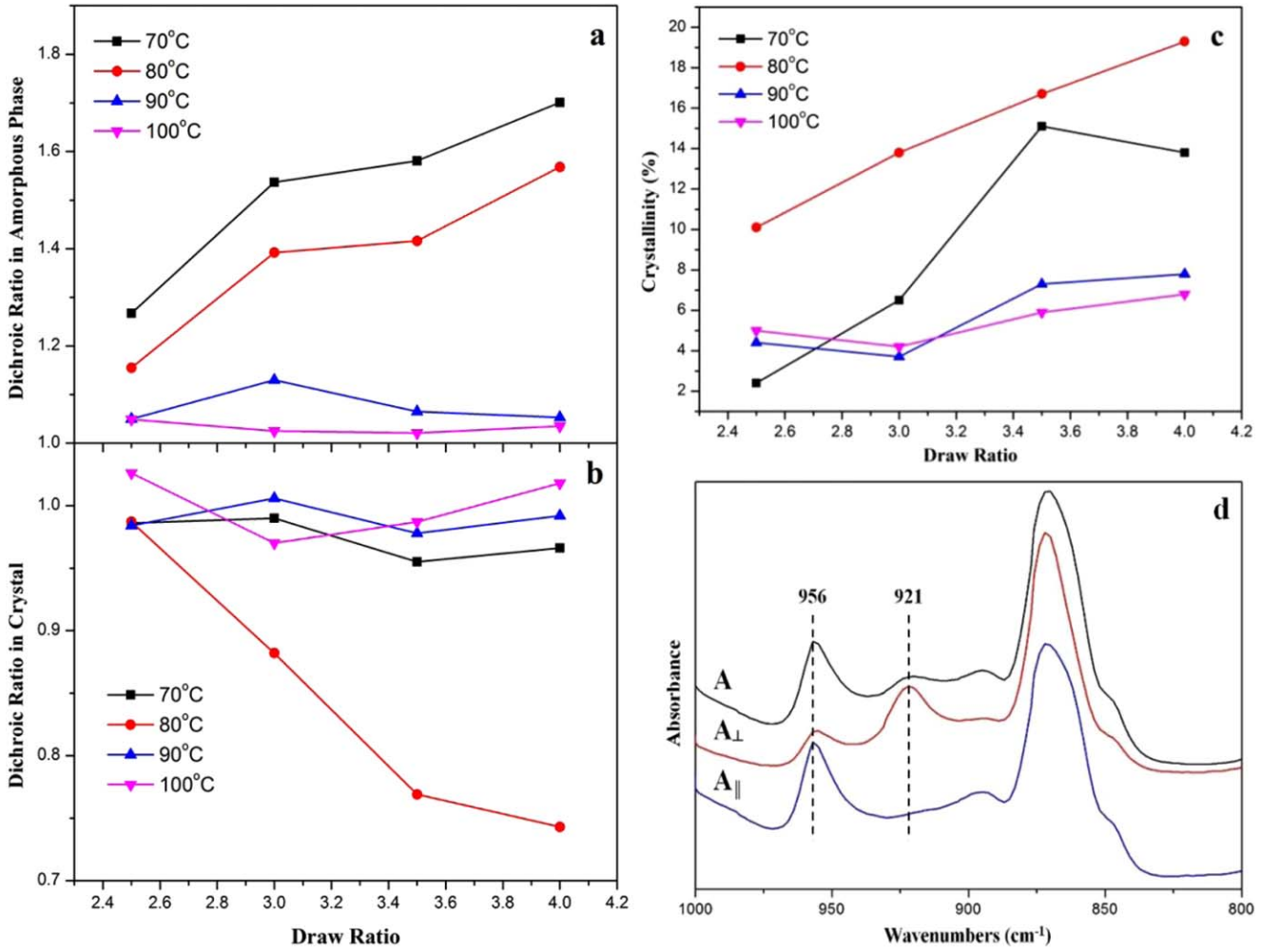

Figure 3. Orientation degree of film changes versus DR measured with FTIR spectroscopy. The films were drawn at various T_d values and at a draw rate of 5 mm/min: (a) amorphous phase, (b) crystal phase, (c) crystallinity degree of films measured with DSC, and (d) FTIR spectra of a PLA film drawn at $T_d = 80°C$ to a DR of 4 measured under parallel and perpendicular polarization in the region $1000 - 800\ cm^{-1}$. [Color figure can be viewed in the online issue, which is available at wileyonlinelibrary.com.]

a DR of 4 became lower relative to that at a DR of 3.5, as shown in Figure 3(c). When the crystallites induced during deformation and existing in the drawn PLA films performed as nucleating agents during heating process, the T_{cc}'s of the drawn film at a DR of 4 should have been higher than that at a DR of 3.5, but this assumption was opposite to the results given in Figure 2(a). So, the decrease in T_{cc} was indeed caused by the cold crystallization of oriented chains in the amorphous phase. Evidently, the variation tendency of the amorphous orientation degree as a function of DR was consistent with that of the T_{cc}'s, as shown in Figure 2(a,b), for the films drawn at 70 and 80°C. However, at T_d's of 90 and 100°C, the amorphous orientation degrees of the chains remained stable, and T_{cc} performed the same. This means that at relatively higher T_d's, 90 and 100°C, the amorphous orientation of the chains could hardly form at a draw rate of 5 mm/min. As shown in Figure 3(b), the crystalline orientation got stronger with increasing DR, obviously only for the film drawn at a T_d of 80°C (from 0.987 to 0.743). However, at T_d's of 70, 90, and 100°C, the crystalline orientation degrees had no regular character.

Similar to those of other semicrystalline polymers, the crystallization behavior of PLA consisted of nucleation and crystal growth. The maximum overall speed of crystallization of PLA in the quiescent melt emerged at about 100°C, as shown in Figure 4. However, as shown in Figure 3(c), the crystallinity increased obviously with increasing DR at a low T_d (70 or 80°C); this indicated that the optimum crystallization temperature for PLA with a draw rate of 5 mm/min was around 80°C but not 100°C. We speculated that strain had a strong influence on the crystallization mechanism of the PLA matrix.

According to the previous results, we made an assumption about the process of strain-induced crystallization as follows. The PLA chains were driven to be oriented by stretching and then arranged into the lattice. However, the relaxation, the instinct of polymer chains, prevented the process of orientation.

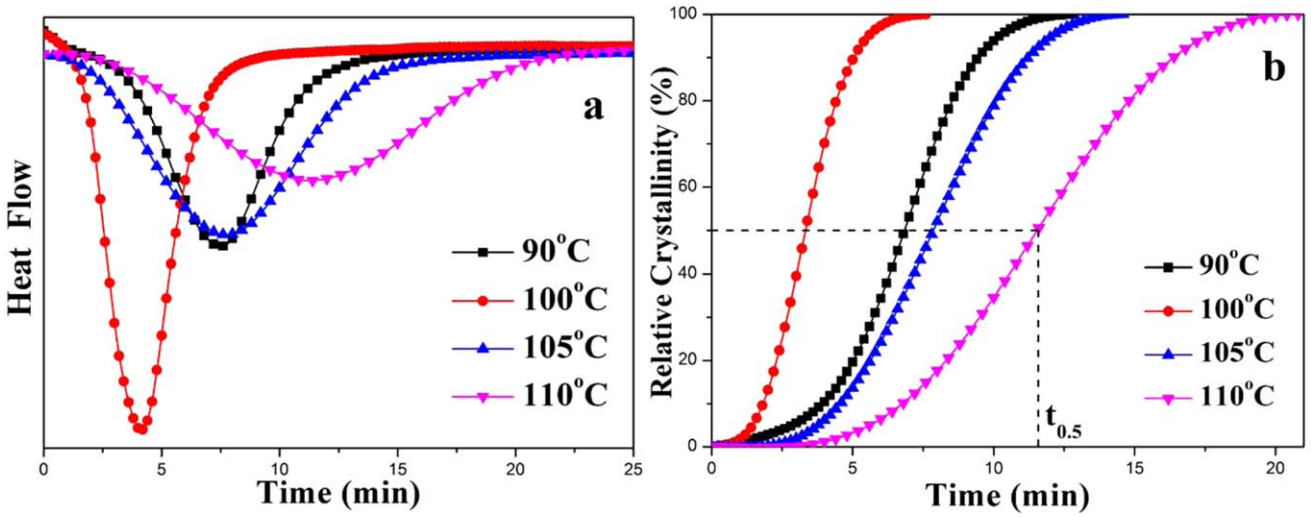

Figure 4. (a) DSC heat flow as a function of time at isothermal crystallization temperatures ranging from 90 to 110°C and (b) relative crystallinity from the DSC test as a function of time. And the $t_{0.5}$ in Fig. 4b means the half-crystallization time of PLA. [Color figure can be viewed in the online issue, which is available at wileyonlinelibrary.com.]

In other words, strain-induced crystallization above the T_g of PLA was the result of the competition between the orientation and relaxation of chains. As is well known, the relaxation rate of PLA chains were accelerated with increasing temperature. Therefore, the crystallinity of the drawn PLA film hardly increased at high temperatures ($T_d = 90$ or 100°C) because the relaxation rate was much higher than that of the orientation caused by stretching at a draw rate of 5 mm/min. However, the crystallinities of the films drawn at 80°C were higher than those drawn at 70°C; this was not completely consistent with the relaxation theory discussed for high temperatures. The key point was that although relaxation was unfavorable for chain orientation and crystallization, to some extent, the mobility of chains was still necessary for arrangement into the lattice. The mobility of chains was too low at 70°C to arrange into the lattice, so the strain-induced crystallization was not as perfect as that at 80°C. In particular, at a T_d of 80°C, the rates of orientation and the relaxation of the chains obtained an optimum balance point for crystallization. All of the previous evidence proves that both the crystallization and crystalline/amorphous orientation could be induced by stretching at temperatures higher than the T_g of PLA when the orientation and relaxation rate of the chains were suitable.

Changing Tendency of Crystallization and Orientation with Various Draw Rates Ranging from 5 to 40 mm/min

When the assumption about the strain-induced crystallization process discussed previously is right, the stronger intensity of stretching should be better for the formation of crystals and orientation during deformation. In another word, the strain-induced crystallization and orientation should work easier with a higher draw rate at a certain T_d. According to the work mentioned previously, 80°C seemed to be the optimum temperature for the formation of strain-induced crystallites in the PLA film. Then, at a fixed T_d of 80°C and a DR of 4, draw rates ranging from 5 to 40 mm/min were used to explore the orientation and crystallization of the PLA film. The DSC heating curves of films drawn at different rates are shown in Figure 5(a). Notably, T_{cc} shifted to lower temperatures (from 83.7 to 76.9°C) with increasing draw rate; this confirmed that the PLA chains in the amorphous phase became more regular during the extension process. The double melting peaks are discussed later. As shown in Figure 5(b), the amorphous/crystalline orientation degree became stronger (from 1.568 to 1.864 and from 0.743 to 0.598, respectively) with increasing draw rate from 5 to 40 mm/min. The POM micrographs shown in Figure 5(c,d) demonstrate the crystalline orientation degree was enhanced significantly with increasing draw rate. Moreover, the crystallinity increased from 19.3 to 28.1% with increasing draw rate. Thereby, we concluded that the strain-induced crystallization and orientation increased monotonically with increasing draw rate.

To verify the relationship between the crystal form and draw rate, X-ray diffraction was used to measure films drawn with different draw rates at a T_d of 80°C, and the curves are shown in Figure 6. At a draw rate of 5 mm/min, only the reflection from the (203) and (110/200) planes characteristic of the α phase, corresponding to 2θ angles of 22.3 and 16.4°, respectively, are observed. In the meanwhile, only the reflection from the (110/200) plane characteristic of the α phase was observed at higher draw rates of 10, 20, and 40 mm/min. So, the double melting peak in the DSC diagram of the film drawn at 80°C at a draw rate of 40 mm/min, as shown in Figure 5(a), was attributed to the melting of the crystallites that formed through melt recrystallization. Therefore, no crystal form transition occurred during deformation.

To determine whether the effective enhancement of strain worked on the formation of the crystallite and orientation at T_d's of 70, 90, and 100°C at draw rates ranging from 5 to 40 mm/min, more information about the chain orientation should be obtained.

The crystallinity and orientation degrees of the films drawn at different temperatures and measured by DSC and FTIR

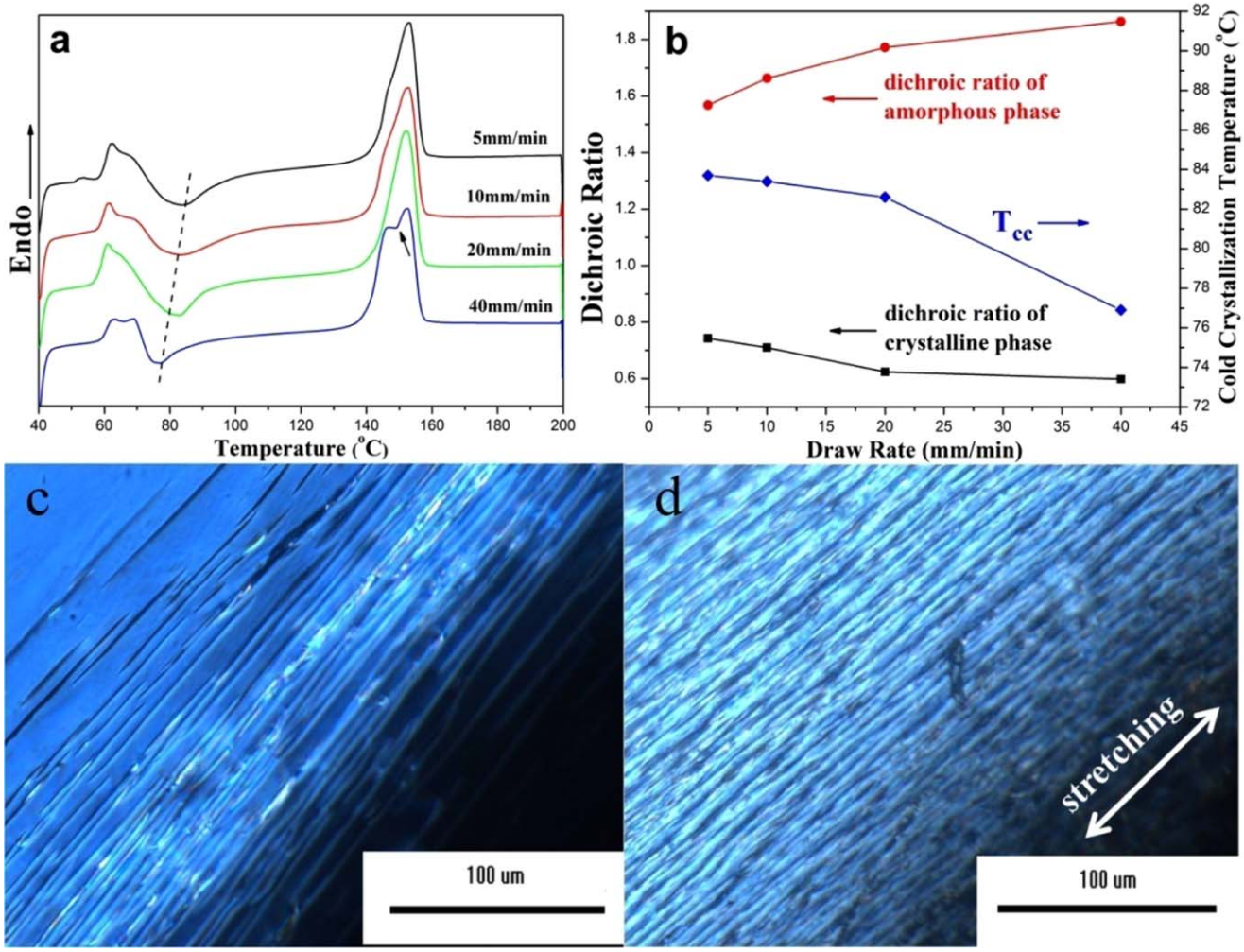

Figure 5. (a) DSC heating curves, (b) orientation degree and cold temperature of PLA films drawn at different draw rates to a DR of 4 at a fixed T_d of 80°C, and (c,d) POM micrographs of PLA films drawn at 80°C to a DR of 4 at draw rates of 5 and (d) 40 mm/min, respectively. [Color figure can be viewed in the online issue, which is available at wileyonlinelibrary.com.]

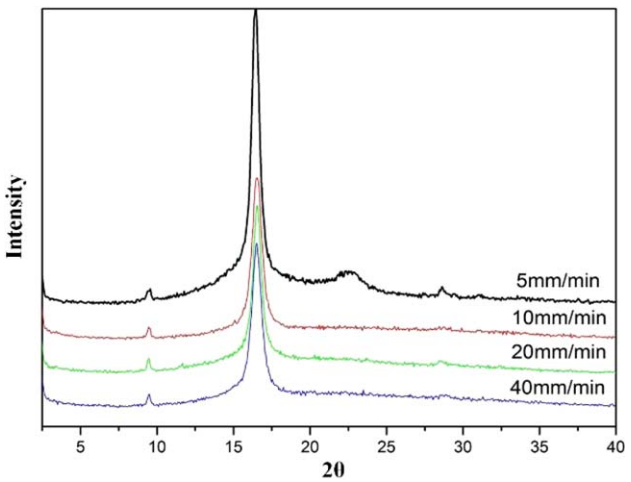

Figure 6. X-ray diffraction patterns measured at room temperature for PLA films drawn at 80°C and various draw rates to a DR of 4. [Color figure can be viewed in the online issue, which is available at wileyonlinelibrary.com.]

spectroscopy, respectively, are shown in Figure 7 and Table III. Unfortunately, the regular increase in the crystallinity emerging at a T_d of 80°C could not recur at T_d's of 70, 90, or 100°C. No obvious crystallite or orientation was observed in the PLA films drawn at a T_d of 100°C within the test range of the draw rate in this study. However, something different was also exhibited here: (1) the crystallinity was significantly enhanced when the draw rate went beyond 20 mm/min at a T_d of 90°C, and (2) the crystallinity of the film drawn at a T_d of 70°C achieved a maximum at a draw rate of 10 mm/min and then decreased continuously with increasing draw rate.

The effects of the draw rate on the crystalline and amorphous orientations are shown in Figure 7(b). At a T_d of 70°C, the amorphous orientation degree in drawn PLA film increased with increasing draw rate and started to decrease when the draw rate increased up to 20 mm/min. The crystalline orientation degree showed tiny growth with increasing draw rate, as shown in the inset in Figure 7(b). At a T_d of 80°C, the crystalline (from 0.743 to 0.598) and amorphous orientation degrees

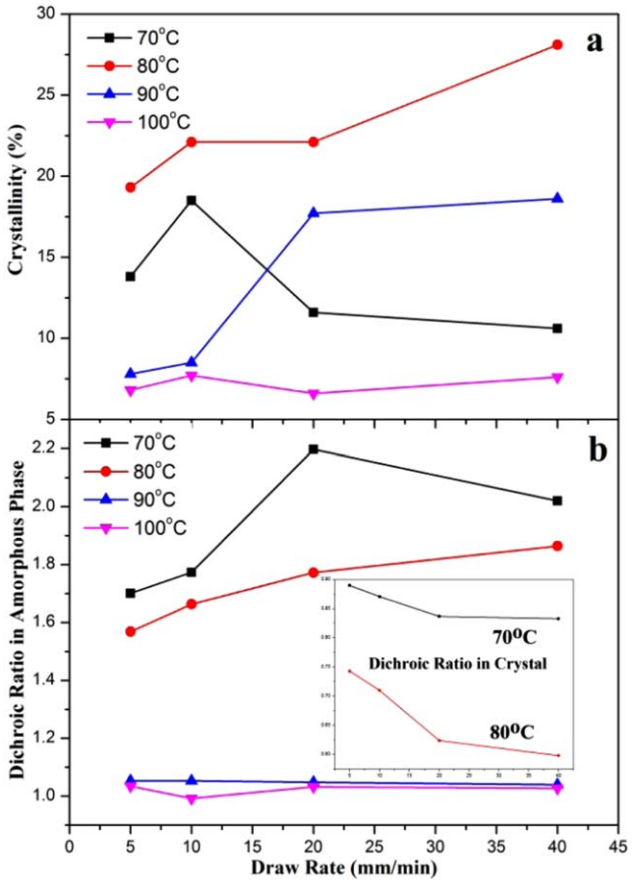

Figure 7. (a) Crystallinity degree and (b) orientation degree in the amorphous phase of PLA films drawn at various T_d values and different draw rates to a DR of 4. [Color figure can be viewed in the online issue, which is available at wileyonlinelibrary.com.]

developed rapidly with increasing draw rate. It was interesting to find that the crystallinity increased significantly, but no obvious orientation was observed in the drawn PLA film at a draw rate of 20 mm/min at a T_d of 90°C. We should disclose that the mechanisms of strain-induced crystallization and orientation were similar, but different suitable conditions in stretching were needed. These phenomena were explained from the perspective of chain movement as follows.

Mechanism of the Chain Motion Mode

The strain-induced crystallization and orientation (amorphous and crystalline) resulted from the competition of the orientation caused by stretching and the relaxation of chains under certain temperature conditions. To discuss this expediently, R_{or} is defined as the ratio between the rates of orientation and relaxation at a certain temperature. The motion modes of the chains were divided into four types related to R_{or}, as shown in Figure 8. At a T_d of 100°C, the PLA chains were activated, and the relaxation rate was much faster than the orientation rate caused by strain. This means that when R_{or} was small, any oriented chains induced by stretching relaxed instantly. No crystallite or orientation could be obtained (within the intensity of the strain and draw rate used here), as shown in Figure 7, and the chains acted in mode I, as shown in Figure 8, during the deformation. Then, at a T_d of 90°C, with the reduction of the relaxation rate, R_{or} became larger than that at 100°C, although it was still not big enough. At a draw rate of 5–10 mm/min, the PLA chains still acted in mode I, no crystallite or orientation could be reserved after unloading. The orientation rate of the PLA chains were enhanced with increasing draw rate, and when the draw rate was above 20 mm/min, the chains acted in mode II, where the PLA chains were arranged into a lattice without being instantly relaxed. Although the amorphous orientation was formed with a draw rate beyond 20 mm/min, the chain relaxation rate was still large enough to destroy the orientation immediately after unloading, so only crystallites induced by strain remained (shown in Figure 7). We believe that the motion mode of chains transformed from I to II at a draw rate of 20 mm/min at a T_d of 90°C. When T_d was 80°C, R_{or} was located in a suitable range, where the chains moved like mode III, as shown in Figure 8. We found that amorphous and crystalline orientations were then obtained. With increasing draw rate, the amorphous chains were oriented better. When the regularity of the oriented amorphous chains achieved a certain criticality, these oriented chains were arranged into lattice; then, the lamellae oriented along the draw direction were obtained. The chain relaxation still existed at 80°C but not more severe than those at 90 and 100°C. So, the amorphous and crystalline orientations could be reserved after unloading. The sketching of the PLA chains acting in mode III were confirmed by the results shown in Figure 5. When T_d was set as 70°C, R_{or} increased further. However, in contrast to that at 80°C, the mobility of the matrix chains was too weak. So, only some short chains could catch the deformation and orient along the draw direction. When the draw rate was set as 10 mm/min, when the crystallinity of the drawn film achieved the maximum, the chains of PLA acted in mode III. However, most entangled long chains remained

Table III. DSC and FTIR Parameters of the Films Drawn to a DR of 4

	X_c (%)				Dichroic ratio in the amorphous phase			
Draw rate (mm/min)	5	10	20	40	5	10	20	40
T_d (°C)								
70	13.8	18.5	11.6	10.6	1.701	1.773	2.197	2.02
80	19.3	22.1	22.1	28.1	1.568	1.663	1.772	1.864
90	7.8	8.5	17.7	18.6	1.053	1.053	1.048	1.04
100	6.8	7.7	6.6	7.6	1.035	0.992	1.032	1.027

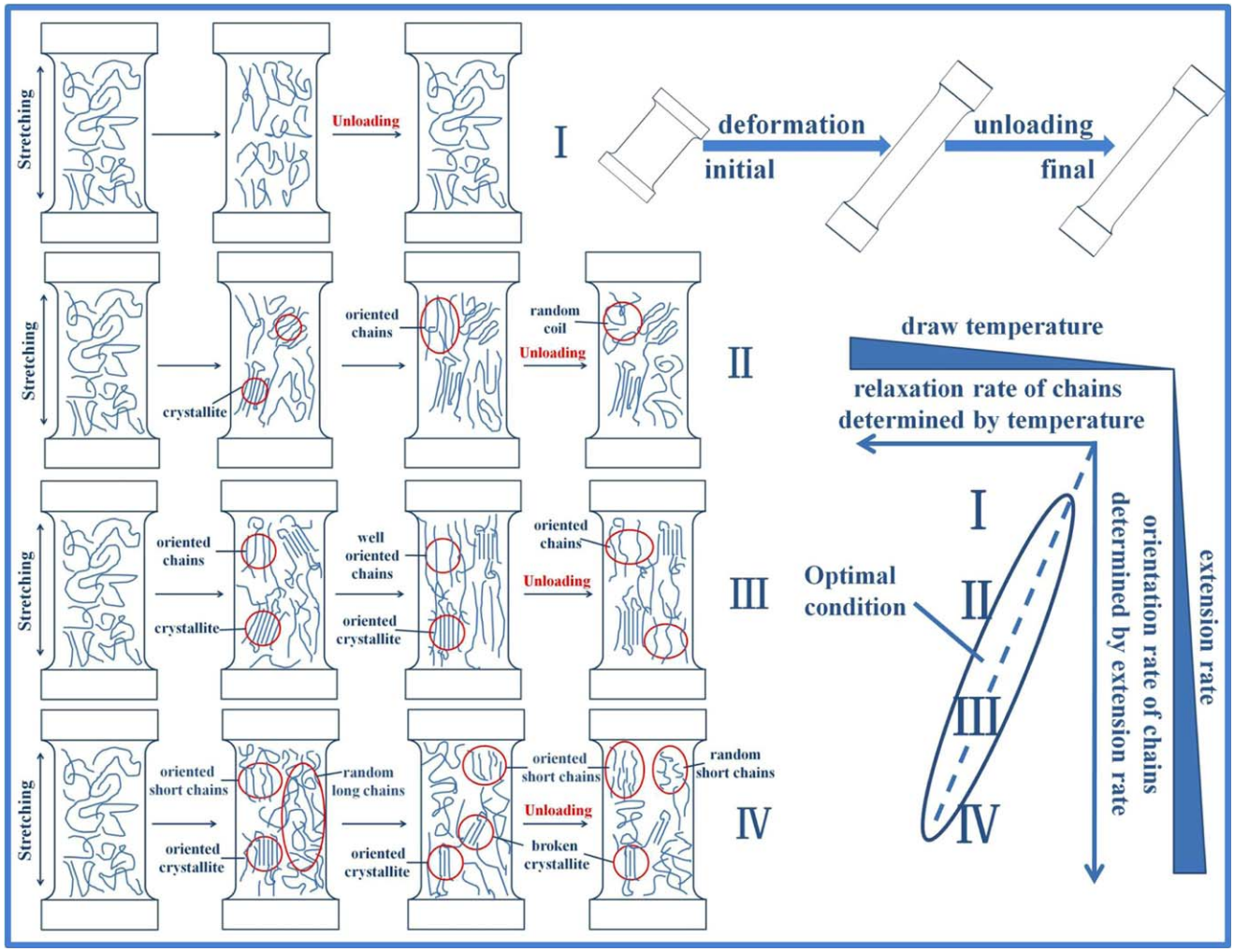

Figure 8. Motion mode of PLA chains determined at different temperatures and draw rates. [Color figure can be viewed in the online issue, which is available at wileyonlinelibrary.com.]

random because of the poor mobility at 70°C. With increasing draw rate, some oriented shorter chains in the amorphous phase formed quickly. Then, the lamellae orienting along the draw direction could be obtained. The higher level of draw rate led to the formation of the higher oriented crystalline phase. So, there were not enough long chains arranging into the lattice; moreover, the crystallites were not as regular as those formed at a T_d of 80°C. Moreover, there also existed some chains not totally ranging into the lattice, and the amorphous segments of these chains entangled with other amorphous chains. With a higher level of draw rate, the heavier pulling of these entangled chains broke the partial crystallites formed previously. This resulted in a decrease in the crystallinity when the draw rate was beyond 10 mm/min. What is worse, when the intensity of strain increased further, the number of chains that could respond to the strain efficiently to become oriented became fewer and the chains became shorter. The shorter chains had a faster relaxation rate even at a lower temperature, such as 70°C; this resulted in a much more severe damage in the amorphous orientation of chains after unloading. Therefore, a decrease in the amorphous orientation was observed beyond a draw rate of 20 mm/min after the decrease in the crystallinity beyond 10 mm/min, as given in Figure 7(a). In addition, a small increase in the crystalline orientation is shown in the inset of Figure 7(b); this may have been caused by the damage in some crystallites that were not regular enough. Thereby, we are sure that the motion model of the PLA chains was transformed from modes III to IV at a draw rate of 10 mm/min, as shown in Figure 8.

Therefore, we predicted that when the draw rate increased further, the motion mode of the chains at 80°C would transform from mode III to IV, and those at 90 and 100°C would transform from mode I or II to III, even IV. In conclusion, the mechanism that describes the transformation of the motion mode of the PLA chains was the focal point in our study.

CONCLUSIONS

The effects of stretching and temperature on the motion of PLA chains in the films were studied with DSC, FTIR spectroscopy, POM, and X-ray diffraction. We made the following conclusions. The crystallization and orientation of the PLA film could

be significantly enhanced by drawing when R_{or} was located in a suitable range, and both of them were induced by the competition of strain-induced chain orientation and chain relaxation. The motion modes of chains were divided into four types, modes I–IV; this was related to the relationship between the orientation and relaxation rates of the chains. The characters of chain motion in these four modes were as follows:

Mode I: The relaxation rate was much faster than the orientation one, and neither crystallization nor orientation took place.
Mode II: Although the relaxation rate was faster, the crystallization and orientation in the amorphous phase formed during deformation; nevertheless, only the strain-induced crystals could be reserved after unloading.
Mode III: When R_{or} was located in a suitable range, the strain-induced crystallization and orientation seemed to be monophonically enhanced with increasing intensity of the stretching.
Mode IV: The orientation rate was faster than the relaxation rate, and the lamellae and amorphous orientation of the chains that formed during deformation were destroyed successively by the further increasing intensity of the strain. No transformation of the crystal form occurred within the conditions used in this study.

ACKNOWLEDGMENTS

This work was supported by the National Natural Science Foundation of China (contract grant numbers 51033003 and 51421061).

REFERENCES

1. Auras, R.; Harte, B.; Selke, S. *Macromol. Biosci.* **2004**, *4*, 835.
2. Mallet, B.; Lamnawar, K.; Maazouz, A. *Polym. Eng. Sci.* **2014**, *54*, 840.
3. Li, H.; Huneault, M. A. *J. Appl. Polym. Sci.* **2011**, *122*, 134.
4. Choi, Y. J.; Choung, S. K.; Hong, C. M.; Shin, I. S.; Park, S. N.; Hong, S. H.; Park, H. K.; Park, Y. H.; Son, Y.; Noh, I. *J. Biomed. Mater. Res. A* **2005**, *75*, 824.
5. Lim, L. T.; Auras, R.; Rubino, M. *Prog. Polym. Sci.* **2008**, *33*, 820.
6. Rasal, R. M.; Janorkar, A. V.; Hirt, D. E. *Prog. Polym. Sci.* **2010**, *35*, 338.
7. Liu, H. Z.; Zhang, J. W. *J. Polym. Sci. Part B: Polym. Phys.* **2011**, *49*, 1051.
8. Zhang, Y. Q.; Wang, Z. K.; Jiang, F.; Bai, J.; Wang, Z. G. *Soft Matter* **2013**, *9*, 5771.
9. Kale, G.; Auras, R.; Singh, S. P.; Narayan, R. *Polym. Test.* **2007**, *26*, 1049.
10. Drumright, R. E.; Gruber, P. R.; Henton, D. E. *Adv. Mater.* **2000**, *12*, 1841.
11. Garlotta, D. *J. Polym. Environ.* **2001**, *9*, 63.
12. Dorgan, J. R.; Janzen, J.; Clayton, M. P.; Hait, S. B.; Knauss, D. M. *J. Rheol.* **2005**, *49*, 607.
13. Cooper-White, J. J.; Mackay, M. E. *J. Polym. Sci. Part B: Polym. Phys.* **1999**, *37*, 1803.
14. Dorgan, J. R.; Williams, J. S.; Lewis, D. N. *J. Rheol.* **1999**, *43*, 1141.
15. Chen, X.; Kalish, J.; Hsu, S. L. *J. Polym. Sci. Part B: Polym. Phys.* **2011**, *49*, 1446.
16. Li, H. B.; Huneault, M. A. *Polymer* **2007**, *48*, 6855.
17. Cabedo, L.; Feijoo, J. L.; Villanueva, M. P.; Lagaron, J. M.; Gimenez, E. *Macromol. Symp.* **2006**, *233*, 191.
18. He, D.; Wang, Y.; Shao, C.; Zheng, G.; Li, Q.; Shen, C. *Polym. Test.* **2013**, *32*, 1088.
19. Rangari, D.; Vasanthan, N. *Macromolecules* **2012**, *45*, 7397.
20. Lee, J. K. W. *Eur. Polym. J.* **2001**, *37*, 907.
21. Young, M. T. A. R. *J. Biomacromolecules* **2006**, *7*, 2575.
22. Delpouve, N.; Stoclet, G.; Saiter, A.; Dargent, E.; Marais, S. *J. Phys. Chem. B* **2012**, *116*, 4615.
23. Zhang, J.; Tashiro, K.; Domb, A. J.; Tsuji, H. *Macromol. Symp.* **2006**, *242*, 274.
24. Takahashi, K.; Sawai, D.; Yokoyama, T.; Kanamoto, T.; Hyon, S.-H. *Polymer* **2004**, *45*, 4969.
25. Zhang, X.; Schneider, K.; Liu, G.; Chen, J.; Brüning, K.; Wang, D.; Stamm, M. *Polymer* **2011**, *52*, 4141.
26. Zhang, X.; Schneider, K.; Liu, G.; Chen, J.; Brüning, K.; Wang, D.; Stamm, M. *Polymer* **2012**, *53*, 648.
27. Liu, H.; Chen, N.; Fujinami, S.; Louzguine-Luzgin, D.; Nakajima, K.; Nishi, T. *Macromolecules* **2012**, *45*, 8770.
28. Stoclet, G.; Seguela, R.; Lefebvre, J. M.; Elkoun, S.; Vanmansart, C. *Macromolecules* **2010**, *43*, 1488.
29. Stoclet, G.; Séguéla, R.; Lefebvre, J. M.; Li, S.; Vert, M. *Macromolecules* **2011**, *44*, 4961.
30. Stoclet, G.; Seguela, R.; Lefebvre, J. M.; Rochas, C. *Macromolecules* **2010**, *43*, 7228.
31. Stoclet, G.; Seguela, R.; Vanmansart, C.; Rochas, C.; Lefebvre, J. M. *Polymer* **2012**, *53*, 519.
32. Fischer, E.; Sterzel, H. J.; Wegner, G.; Kolloid-Z, Z. *Polym.* **1973**, *251*, 980.
33. Mahendrasingam, A.; Blundell, D. J.; Parton, M.; Wright, A. K.; Rasburn, J.; Narayanan, T.; Fuller, W. *Polymer* **2005**, *46*, 6009.